ACTA ASTRONOMICA
Vol. **66** (2016) pp. 255–267

OGLE Collection of Star Clusters. New Objects in the Outskirts of the Large Magellanic Cloud*

M. Sitek[1], M.K. Szymański[1], D.M. Skowron[1], A. Udalski[1], Z. Kostrzewa-Rutkowska[2,3], J. Skowron[1], P. Karczmarek[1], M. Cieślar[1], Ł. Wyrzykowski[1], S. Kozłowski[1], P. Pietrukowicz[1], I. Soszyński[1], P. Mróz[1], M. Pawlak[1], R. Poleski[1,4] and K. Ulaczyk[1,5]

[1] Warsaw University Observatory, Al Ujazdowskie 4, 00-478 Warszawa, Poland
[2] SRON Netherlands Institute for Space Research, Sorbonnelaan 2, 3584 CA Utrecht, The Netherlands
[3] Department of Astrophysics/IMAPP, Radboud University Nijmegen, P.O. Box 9010, 6500 GL Nijmegen, The Netherlands
[4] Department of Astronomy, Ohio State University, 140 W. 18th Ave., Columbus, OH 43210, USA
[5] Department of Physics, University of Warwick, Gibbet Hill Road, Coventry, CV4 7AL, UK
e-mail:(msitek, msz)@astrouw.edu.pl

Received September 22, 2016

ABSTRACT

The Magellanic System (MS), consisting of the Large Magellanic Cloud (LMC), the Small Magellanic Cloud (SMC) and the Magellanic Bridge (MBR), contains diverse sample of star clusters. Their spatial distribution, ages and chemical abundances may provide important information about the history of formation of the whole System. We use deep photometric maps derived from the images collected during the fourth phase of the Optical Gravitational Lensing Experiment (OGLE-IV) to construct the most complete catalog of star clusters in the Large Magellanic Cloud using the homogeneous photometric data. In this paper we present the collection of star clusters found in the area of about 225 square degrees in the outer regions of the LMC. Our sample contains 679 visually identified star cluster candidates, 226 of which were not listed in any of the previously published catalogs. The new clusters are mainly young small open clusters or clusters similar to associations.

Key words: *Catalogs – Surveys – Magellanic Clouds – Galaxies: clusters: general*

1. Introduction

The Magellanic System is an ideal astrophysical laboratory for studying the structure and evolution of galaxies. It is located close enough to the Galaxy so that millions of stars can be easily resolved. This can be used in a range of scientific

*Based on observations obtained with the 1.3-m Warsaw telescope at the Las Campanas Observatory of the Carnegie Institution for Science.

projects exploring stellar populations, their evolution, ages, metallicity (Jacyszyn-Dobrzeniecka *et al.* 2016, Skowron *et al.* 2014). One of the methods for such studies is the investigation of star clusters. The Large Magellanic Cloud contains a large sample of these systems. The spatial distribution of clusters, their age, chemical composition, structural parameters and dynamical evolution may provide valuable information about the LMC formation history. The Magellanic System has a very rich and diverse structure. The positions of centroids of both Clouds depend on which stellar population is used for their estimation (Cioni, Habing and Israel 2000, Deb and Singh 2014). Moreover, the Magellanic Clouds look asymmetrical, with denser parts located toward the Bridge (Klein *et al.* 2014, Scowcroft *et al.* 2016). Analysis of the spatial distribution of the star clusters in the MS enables the comparison to the general stellar populations. This may give some hints of what caused the asymmetry of the LMC and the SMC. The correlation between age, size, metallicity and spatial distribution can bring new information about the MS history (Palma *et al.* 2016, Piatti *et al.* 2014). To make all these studies possible, however, a complete collection of star clusters is needed, derived from homogeneous observational data, possibly from a single photometric survey.

So far, the largest catalog of extended objects (excluding background galaxies) in the Magellanic System was published by Bica *et al.* (2008) and contains a compilation of all the previously published catalogs. The most important contribution to this sample was due to the catalog based on the OGLE-II data published by Pietrzyński *et al.* (1999). That catalog, however, covered only the central part of the LMC: 5.8 square degrees – only 3% of the area observed during the current OGLE-IV phase (Udalski, Szymański and Szymański 2015).

The parameters (such as size, age, metallicity) of some clusters listed in the Bica catalog (Bica *et al.* 2008) were estimated by several groups, including Glatt, Grebel and Koch (2010), Palma *et al.* (2016), Choudhury, Subramaniam and Piatti (2015) and Piatti *et al.* (2002, 2003ab, 2009, 2014, 2015). The OGLE survey data were also used for this purpose, first by Pietrzyński and Udalski (2000) using OGLE-II data (Udalski, Kubiak and Szymański 1997) and recently, by Nayak *et al.* (2016), using OGLE-III data (Udalski *et al.* 2008).

The OGLE-IV survey covers practically the entire Magellanic System including both galaxies and the Magellanic Bridge (about 650 square degrees). The large collection of high resolution individual images enabled construction of deep images of the entire region with a depth comparable to images collected by a 4-m class telescope. Uniform OGLE-IV photometric data provide a unique, homogeneous data set for the search of star clusters and associations. It will allow us to create a complete catalog of star clusters in the MS and the determination of their basic parameters.

This paper presents the first part of the catalog based on the OGLE-IV data. The central part of the LMC has already been observed or analyzed by many other projects so we decided to start our exploration with the outer parts of the galaxy.

We have found 679 star clusters in the outer regions of the LMC. Among those, 226 objects were not listed in any of the previous catalogs, 438 objects were listed in the Bica catalog and 15 objects were listed in the Dark Energy Survey (DES) publication (Pieres *et al.* 2016). As some extended objects cannot be unambiguously classified, we have performed a cross-match of our sample to both star clusters and associations from the Bica catalog. Almost all known objects which were in the area of the analyzed OGLE fields were detected by our algorithm, proving the effectiveness of algorithm and the completeness of the sample. There are five Bica objects which we do not see in our images and one DES object which is located in the gap between the OGLE subfields.

2. Observations and Data Reduction

The photometric data of the LMC fields analyzed in this paper come from the images gathered during the first five years (2010–2015) of the fourth phase of the OGLE project (OGLE-IV, Udalski, Szymański and Szymański 2015). The project has been conducted on the 1.3-meter Warsaw Telescope at the Las Campanas Observatory, equipped with the 32-chip mosaic CCD camera, covering 1.4 square degree field with $0.''26$ per pixel scale (see the aforementioned paper for the details of the OGLE-IV hardware setup, observational strategy and photometric reductions pipeline).

We have used the "deep photometric maps" – catalogs of all objects detected on the deep images of all observed fields. The deep photometric maps for the OGLE-IV have not been published yet, but they were prepared in a similar way to those published for the OGLE-III phase of the project (see Udalski *et al.* 2008 for the LMC OGLE-III data). The main, crucial difference is that the OGLE-IV maps are much deeper, as the template images were constructed, for the *I*-band, by stacking up to 100 images taken in the best photometric weather conditions. For all 213 observed LMC fields, the number of the stacked images used for the templates is between 61 and 100 (90 on average), depending on the overall number of good seeing individual images available for a given field. For *V*-band, which is observed less frequently, the templates were constructed from 4 to 100 individual images with the mean value of 19. For comparison, the templates for 116 OGLE-III LMC fields were constructed of at most 10 images. We refer to the OGLE-IV maps used in this paper as "deep photometric maps" in order to distinguish them from the preliminary maps constructed for internal use in 2012 from much "shallower" templates. The catalog data include the coordinates of objects, calibrated V and I mean magnitudes, their errors, $V-I$ color index.

Every observed field is divided into 32 subfields according to the setup of the mosaic CCD camera chips. Photometry reductions, databases and photometric maps are done independently for each subfield.

The star detection limit of the deep photometric maps of the LMC reaches $I \approx 23.5$ mag and $V \approx 24$ mag. The maps are complete to about 20.5–21.5 mag in the *I*-

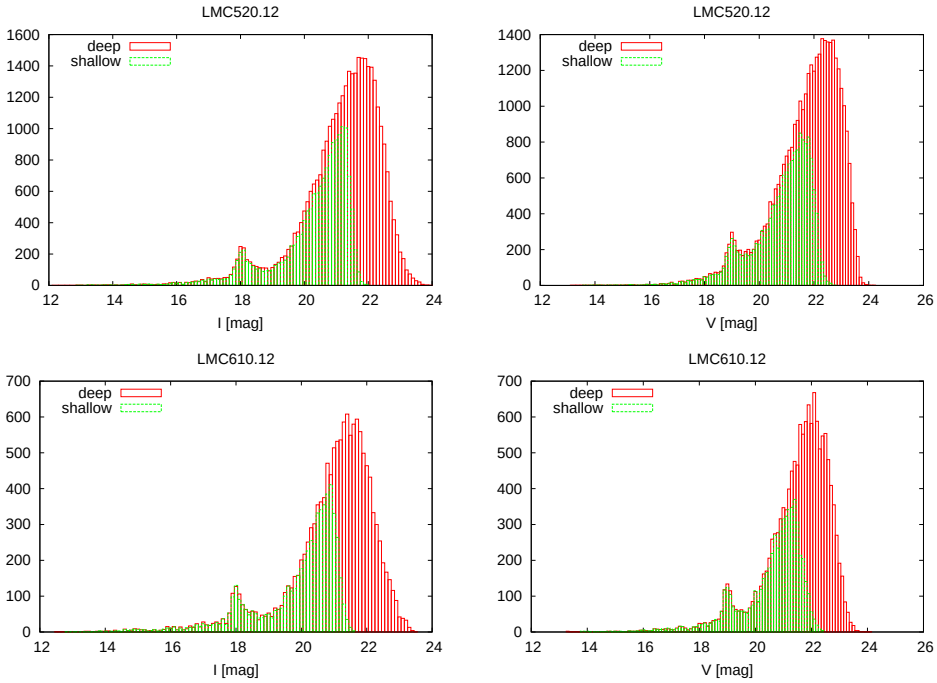

Fig. 1. Histograms of brightness (*left panels* are *I*-band and *right panels* are *V*-band) for two OGLE-IV subfields LMC520.12 (*top panels*) and LMC610.12 (*bottom panels)*.

band and 21.5–22.5 mag in the *V*-band, depending on the location and crowding of the field. These limits are determined from the histograms of the star magnitudes by the estimation of the magnitude where the numbers start to deviate from the systematic growth (Fig. 1). This photometric range should allow us to detect a vast majority of star clusters in the Magellanic System, with a possible exception of the most sparse objects and objects which are located in the gaps between the fields. To obtain stellar magnitudes, the PSF photometry was performed directly on the deep template images, using DOPHOT program (Schechter, Mateo and Saha 1993). This is another important difference to the previously published OGLE photometric maps which were based on the OGLE standard pipeline photometry obtained by using the image difference technique.

3. Search for Clusters

The first attempt to search for star clusters using a fully automated algorithms was undertaken by Bhatia and MacGillivray (1989). They found 284 clusters in a 6 square degrees region toward the North-East end part of the LMC bar, four times more than it was previously known in the observed region. Zaritsky *et al.* (1997) searched for star clusters similarly as Bhatia and MacGillivray but they were using, for the first time, observations from a CCD camera. The result increased the number of identified clusters by about 45% in the central $8^\circ \times 8^\circ$ region of the LMC.

In general, Zaritsky's automated method is based on photometric maps which are divided into small cells. The size of the cell depends on the region crowding – the denser field is the smaller cells are needed. Afterwards the stars are counted in each cell and then the algorithm looks for cells which have more stars than a typical cell (threshold). Zaritsky's method is still in use with small modifications depending on the quality of observations. For example Pietrzyński *et al.* (1999) used this method as well on the OGLE-II data.

Our search for star clusters was based on the deep photometric maps filtered effectively from most artefacts by using only objects detected in both *I*- and *V*-band deep template images. We have divided the LMC region into two parts – the disk

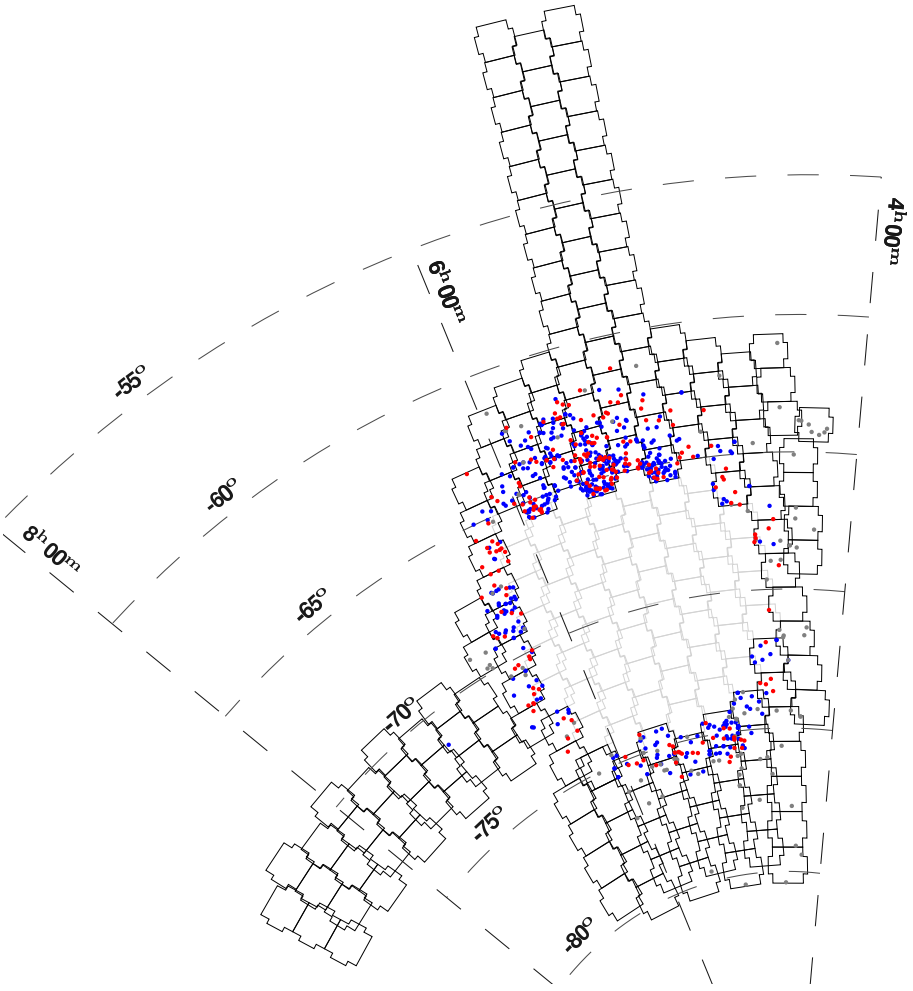

Fig. 2. The OGLE-IV fields in the LMC region. Outer black polygons were analyzed in this paper. Red and blue dots mark the newly discovered and the previously known star clusters, respectively. Gray dots are objects which passed the visual inspection but were rejected by the reliability cut off (see Section 4).

region and the outer part of the LMC. Here, we present the analysis of the fields located outside the LMC disk (Fig. 2). Our method is effective and reliable only in sparse stellar fields. The search method for the densest fields will be described in the next part of the catalog.

The examined area of 225 square degrees contains 165 OGLE-IV fields (5280 single subfields). The analyzed region includes 6 denser fields (LMC513, LMC520, LMC564, LMC73, LMC592, LMC596) located north of declination -65°, to allow full comparison with the DES (Pieres *et al.* 2016) results. All analyzed fields are shown in Fig. 2 marked with black polygons. The gray polygons mark the central LMC fields which have not been analyzed here. The list of all analyzed LMC fields and their central coordinates is available on the Web page together with other supplementary information (see Section 4 for details).

We applied the search method as follows. First, we divided each photometric map into square cells and counted the stars in each cell to create a density map. For each field we prepared three density maps with different cell sizes – 23 pixels ($6''$), 47 pixels ($12''$) and 93 pixels ($24''$). Maps with the smallest cells were suitable for finding the smallest clusters or clusters similar to associations, while the bigger cells were suitable only for globular clusters or large and dense open clusters. Exemplary density maps are presented in Figs. 3 and 4.

Outer regions of the LMC are generally sparse. Still, the stellar density varies significantly, so we divided the density maps into three groups with a different threshold values. The threshold is a value of counts in a cell above which our algorithm selected the denser areas in each subfield. The thresholds were based on median counts in cells with the size of 47 pixels. The first group contained the most dense fields where the value of the median was larger than a half of the value of the maximum count in the field. In this group, we chose the cells with the counts higher than the median values plus one. In the second group we defined the threshold as two times the median value plus two. The third group contains the most sparse fields. In those we selected the cells with counts higher than the half of the maximum value. Those three density groups and their threshold values are defined in Table 1.

T a b l e 1

Cell density groups and their threshold values

group	I $\left(\text{median} > \frac{\text{maximum}}{2}\right)$	II $\left(0 < \text{median} < \frac{\text{maximum}}{2}\right)$	III (median $= 0$)
threshold	median $+ 1$	$2 \times$ median $+ 2$	$\frac{\text{maximum}}{2}$

Median and maximum denote the number of counts in a cell.

The cells with values higher than the threshold which were next to each other were merged to one – the cell with the highest count. The coordinates of this cell were used as the first estimation of the central point of the star concentration in the area.

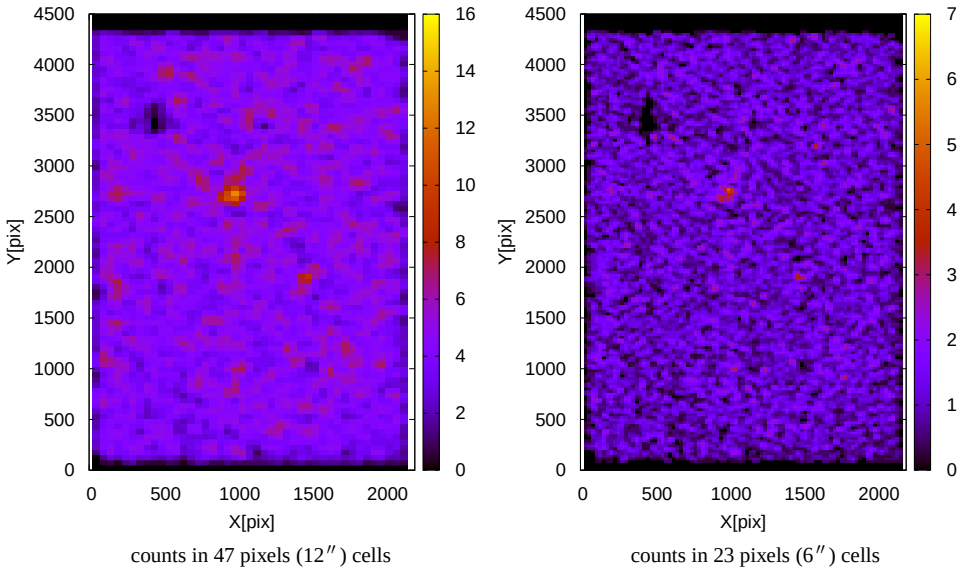

Fig. 3. Stellar density maps of the LMC610.07 field for two different cell sizes. Field contains two clusters: OGLE-LMC-CL-0883, which is located around (1490,1900) and, previously known, OGLE-LMC-CL-1025 (SL873, LW447, KMHK1715) around (1000,2750).

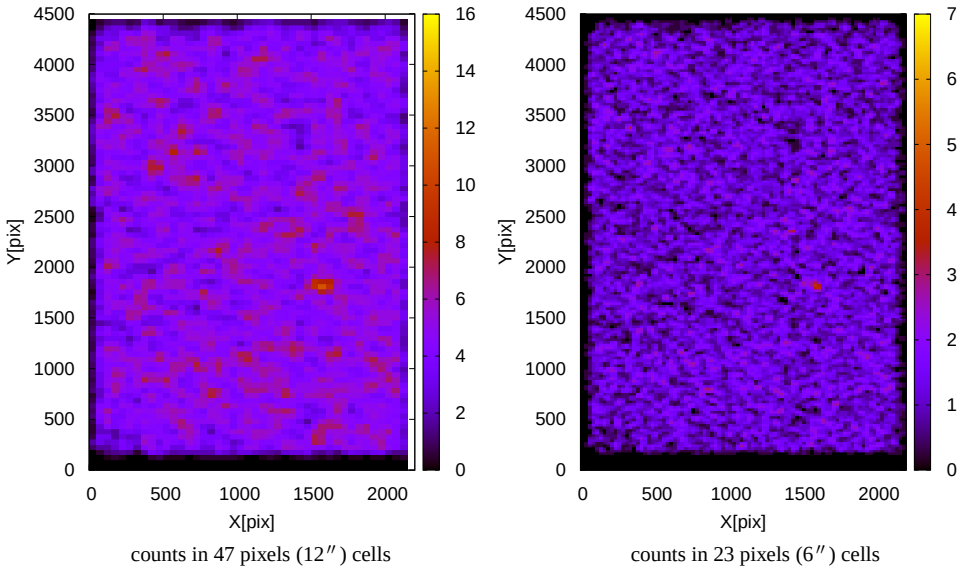

Fig. 4. Stellar density maps of a subfield number LMC582.01 with object OGLE-LMC-CL-0877 located around (1600,1850).

The algorithm yielded almost 6000 candidate areas which were visually inspected by cutting out regions of 400×400 pixels ($1\farcm7 \times 1\farcm7$). For every region we constructed a false-color composition of images taken in *I*- and *V*- band (Fig. 5) and plotted a photometric map with marked brightness and color $(V-I)$ of the stars (see Fig. 6 for a sample plot).

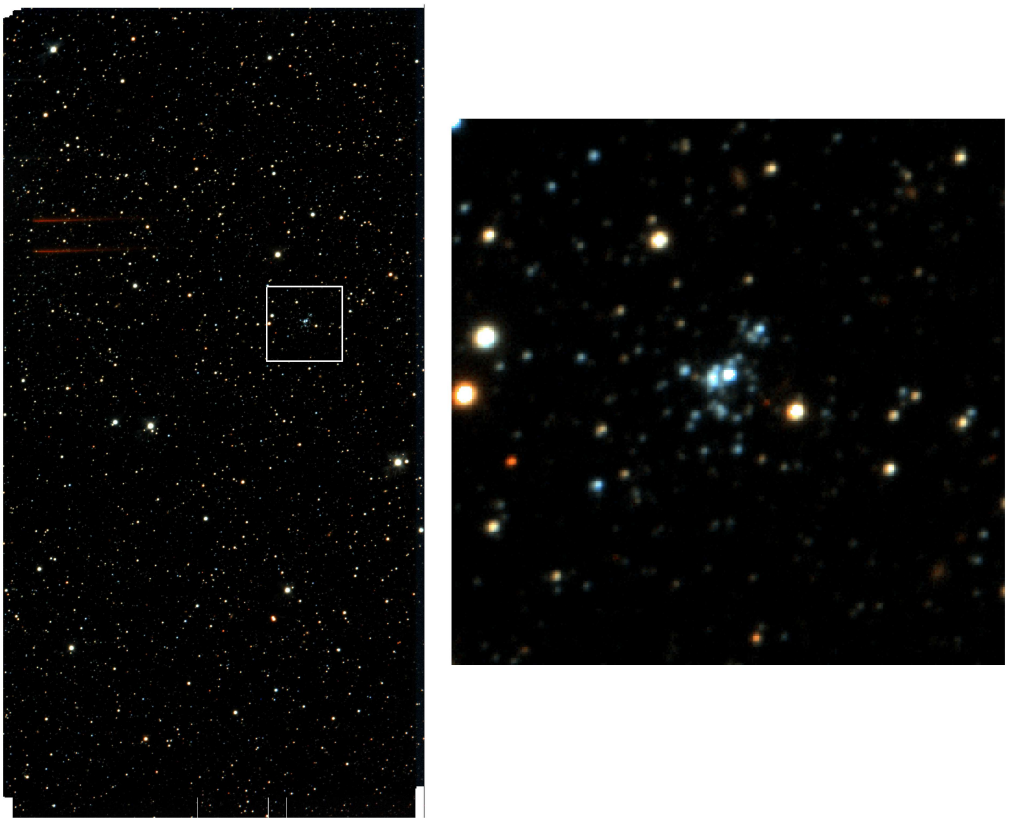

Fig. 5. Color image of the field LMC582.01. White square ($1\farcm7 \times 1\farcm7$) is enlarged in the *right panel*, clearly showing the cluster OGLE-LMC-CL-0877.

Most of the false detections were caused by bright and overexposed stars, background galaxies spuriously detected by the PSF software as groups of stars, and other outliers on the edge of the field. It is worth noting that due to the way of the construction of template images, the quality of the photometry of objects close to the edges of the subfields is worse than in other regions – due to the smaller number of individual components in the template image there.

The visual inspection was based on the density maps, color images, template images in both filters and photometric maps. We compared all seven pictures (three density maps, *I*-band image, *V*-band image, composition of *I*- and *V*- band images, photometric map) for each potential star cluster. If the cluster was visible on all

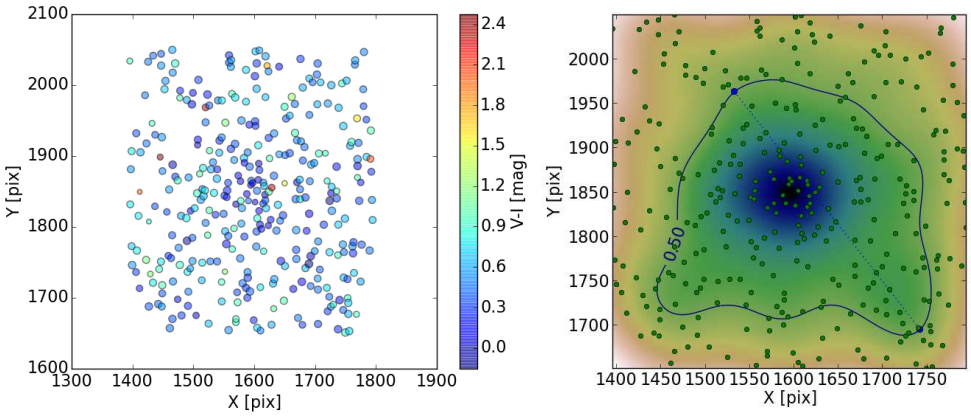

Fig. 6. Deep photometric map of the cluster OGLE-LMC-CL-0877 with the same size as in Fig. 5 – $1\farcm7 \times 1\farcm7$. *Left panel*: size of each point is proportional to the brightness of a star in *I*-band, and the color represents the $V-I$ color of each star. *Right panel*: Deep photometric map with standard KDE distribution which was used to estimate the object's centroid.

of them, the reliability index of detection was set to one, but for each picture not showing any concentration of stars this parameter was reduced by 0.1. If the assigned reliability value was smaller than 0.6, the object was rejected. Of all objects which passed the visual inspection and were assigned the reliability index, 59% received the maximum value of 1, 5% – 0.9, 3% – 0.8, 4% – 0.7 and 6% – 0.6. The remaining 23% with the index less than 0.6 were rejected from the sample. All pictures (images in *V*- and *I*- band, color images and a photometric map) of the accepted star clusters are shown on the Web page (Section 4).

To determine the centroids of the star clusters we used standard Gaussian Kernel Density Estimation (KDE) from the Python scipy.stats library. Firstly, we selected the stars from a 400×400 pixels square around the central point estimated from the densest cell. Then, we computed the coordinates of the maximum value from KDE and again we selected the stars from the square of the same size centered on the point of the KDE maximum value. We repeated the procedure three times to obtain acceptable accuracy of the centroid. The subsequently computed coordinates differ by not more than a few pixels ($\approx 1''$). Exemplary KDE for the object OGLE-LMC-CL-0877 is shown in Fig. 6.

To estimate the approximate size of a star cluster we calculated the average distance from the centroid to the KDE contour line located at half maximum value (normalized to 0.5, see Fig. 6 for a sample contour).

All the centroids were calculated in *XY* coordinates of the field and then converted to equatorial coordinates. Radii are given in arcsec. The parameters are presented in Table 2 for the new objects and in Table 3 for the already known objects.

4. The OGLE Collection of Star Clusters in the Outer Regions of the LMC

We have found 226 new star clusters in the 225 square degrees area of the outer regions of the LMC, based on observations collected by the OGLE-IV survey. All these objects were numbered according to the OGLE-IV naming scheme. The name consists of four parts: the first is the name of the project (OGLE), the second is the abbreviated name of the Large Magellanic Cloud (LMC), the third is the name of the type of the object (CL for star Clusters) and the last part is the number of the object in the OGLE-IV list. To make the numbering consistent with the OGLE-II catalog (Pietrzyński *et al.* 1999), we start it at 0746.

T a b l e 2

New star clusters (excerpt, see web page for full table)

OGLE-IV name	OGLE-IV field	RA	DEC	reliability	$R_{\rm KDE}$
OGLE-LMC-CL-0746	LMC600.16	$5^{\rm h}45^{\rm m}02\overset{\rm s}{.}72$	$-63°48'43\overset{''}{.}0$	1	$49''$
OGLE-LMC-CL-0747	LMC600.18	$5^{\rm h}54^{\rm m}57\overset{\rm s}{.}81$	$-63°29'24\overset{''}{.}4$	1	$42''$
OGLE-LMC-CL-0748	LMC600.22	$5^{\rm h}49^{\rm m}49\overset{\rm s}{.}14$	$-63°36'01\overset{''}{.}6$	0.9	$49''$
OGLE-LMC-CL-0749	LMC600.23	$5^{\rm h}48^{\rm m}29\overset{\rm s}{.}67$	$-63°44'33\overset{''}{.}4$	0.8	$51''$
OGLE-LMC-CL-0750	LMC601.14	$5^{\rm h}47^{\rm m}21\overset{\rm s}{.}41$	$-62°49'41\overset{''}{.}2$	0.6	$55''$
OGLE-LMC-CL-0751	LMC603.05	$6^{\rm h}00^{\rm m}23\overset{\rm s}{.}98$	$-64°53'11\overset{''}{.}7$	1	$37''$
OGLE-LMC-CL-0752	LMC603.10	$6^{\rm h}05^{\rm m}15\overset{\rm s}{.}46$	$-64°33'20\overset{''}{.}1$	0.6	$45''$
OGLE-LMC-CL-0753	LMC603.18	$6^{\rm h}06^{\rm m}34\overset{\rm s}{.}49$	$-64°20'23\overset{''}{.}1$	1	$33''$
OGLE-LMC-CL-0754	LMC603.25	$5^{\rm h}56^{\rm m}16\overset{\rm s}{.}88$	$-64°14'25\overset{''}{.}6$	0.8	$47''$
OGLE-LMC-CL-0755	LMC603.25	$5^{\rm h}56^{\rm m}20\overset{\rm s}{.}46$	$-64°22'19\overset{''}{.}0$	0.6	$40''$
OGLE-LMC-CL-0756	LMC605.16	$5^{\rm h}53^{\rm m}37\overset{\rm s}{.}44$	$-62°12'17\overset{''}{.}2$	0.7	$50''$
OGLE-LMC-CL-0757	LMC606.29	$6^{\rm h}10^{\rm m}50\overset{\rm s}{.}00$	$-63°12'53\overset{''}{.}3$	0.7	$46''$
OGLE-LMC-CL-0758	LMC607.01	$6^{\rm h}17^{\rm m}42\overset{\rm s}{.}12$	$-65°32'53\overset{''}{.}3$	1	$24''$
OGLE-LMC-CL-0759	LMC607.13	$6^{\rm h}11^{\rm m}16\overset{\rm s}{.}44$	$-65°09'42\overset{''}{.}3$	1	$40''$
OGLE-LMC-CL-0760	LMC608.07	$6^{\rm h}10^{\rm m}23\overset{\rm s}{.}58$	$-66°43'03\overset{''}{.}7$	1	$47''$
⋮	⋮	⋮	⋮	⋮	⋮
OGLE-LMC-CL-0957	LMC520.09	$5^{\rm h}34^{\rm m}21\overset{\rm s}{.}84$	$-65°03'35\overset{''}{.}4$	0.8	$49''$
OGLE-LMC-CL-0958	LMC520.10	$5^{\rm h}33^{\rm m}43\overset{\rm s}{.}75$	$-65°10'44\overset{''}{.}4$	0.7	$54''$
OGLE-LMC-CL-0959	LMC520.13	$5^{\rm h}28^{\rm m}17\overset{\rm s}{.}19$	$-65°00'50\overset{''}{.}3$	0.8	$42''$
OGLE-LMC-CL-0960	LMC520.15	$5^{\rm h}26^{\rm m}02\overset{\rm s}{.}62$	$-65°10'14\overset{''}{.}2$	0.8	$51''$
OGLE-LMC-CL-0961	LMC520.15	$5^{\rm h}25^{\rm m}42\overset{\rm s}{.}53$	$-65°06'26\overset{''}{.}0$	1	$49''$
OGLE-LMC-CL-0962	LMC520.16	$5^{\rm h}23^{\rm m}49\overset{\rm s}{.}33$	$-65°08'52\overset{''}{.}4$	0.9	$45''$
OGLE-LMC-CL-0963	LMC520.21	$5^{\rm h}29^{\rm m}41\overset{\rm s}{.}66$	$-64°57'28\overset{''}{.}7$	0.7	$45''$
OGLE-LMC-CL-0964	LMC520.24	$5^{\rm h}26^{\rm m}36\overset{\rm s}{.}81$	$-64°46'53\overset{''}{.}8$	0.8	$46''$
OGLE-LMC-CL-0965	LMC520.25	$5^{\rm h}24^{\rm m}48\overset{\rm s}{.}58$	$-64°48'42\overset{''}{.}0$	0.6	$51''$
OGLE-LMC-CL-0966	LMC520.25	$5^{\rm h}24^{\rm m}29\overset{\rm s}{.}97$	$-64°50'04\overset{''}{.}3$	1	$57''$
OGLE-LMC-CL-0967	LMC520.26	$5^{\rm h}34^{\rm m}28\overset{\rm s}{.}96$	$-64°38'13\overset{''}{.}5$	0.7	$49''$
OGLE-LMC-CL-0968	LMC520.28	$5^{\rm h}31^{\rm m}44\overset{\rm s}{.}22$	$-64°30'55\overset{''}{.}1$	0.8	$50''$
OGLE-LMC-CL-0969	LMC520.29	$5^{\rm h}30^{\rm m}20\overset{\rm s}{.}58$	$-64°32'41\overset{''}{.}3$	0.8	$47''$
OGLE-LMC-CL-0970	LMC520.30	$5^{\rm h}28^{\rm m}31\overset{\rm s}{.}47$	$-64°34'12\overset{''}{.}9$	0.7	$60''$
OGLE-LMC-CL-0971	LMC520.31	$5^{\rm h}26^{\rm m}56\overset{\rm s}{.}80$	$-64°23'20\overset{''}{.}2$	0.6	$49''$

T a b l e 3

Already known star clusters (excerpt, see web page for full table)

OGLE-IV name	OGLE-IV field	name	type from Bica	RA	DEC	R_{KDE}
OGLE-LMC-CL-0972	LMC600.04	LW319, KMHK1439	C	$5^{\mathrm{h}}51^{\mathrm{m}}05\overset{\mathrm{s}}{.}84$	$-64°11'13\overset{''}{.}3$	$41''$
OGLE-LMC-CL-0973	LMC600.05	KMHK1391	C	$5^{\mathrm{h}}49^{\mathrm{m}}02\overset{\mathrm{s}}{.}12$	$-64°20'53\overset{''}{.}6$	$39''$
OGLE-LMC-CL-0974	LMC600.05	SL738, LW314, KMHK1417	C	$5^{\mathrm{h}}50^{\mathrm{m}}05\overset{\mathrm{s}}{.}93$	$-64°09'16\overset{''}{.}9$	$47''$
OGLE-LMC-CL-0975	LMC600.10	KMHK1484	CA	$5^{\mathrm{h}}53^{\mathrm{m}}12\overset{\mathrm{s}}{.}08$	$-63°48'27\overset{''}{.}4$	$42''$
OGLE-LMC-CL-0976	LMC600.11	LW323, KMHK1455	C	$5^{\mathrm{h}}51^{\mathrm{m}}45\overset{\mathrm{s}}{.}50$	$-63°51'19\overset{''}{.}5$	$33''$
OGLE-LMC-CL-0977	LMC600.15	SL710, LW298, ESO86SC32, KMHK1356	C	$5^{\mathrm{h}}47^{\mathrm{m}}02\overset{\mathrm{s}}{.}17$	$-63°52'37\overset{''}{.}5$	$45''$
OGLE-LMC-CL-0978	LMC600.15	BSDL2976	C	$5^{\mathrm{h}}46^{\mathrm{m}}50\overset{\mathrm{s}}{.}44$	$-63°51'24\overset{''}{.}3$	$49''$
OGLE-LMC-CL-0979	LMC600.17	KMHK1530	CA	$5^{\mathrm{h}}56^{\mathrm{m}}08\overset{\mathrm{s}}{.}30$	$-63°38'34\overset{''}{.}6$	$37''$
OGLE-LMC-CL-0980	LMC600.19	SL768, LW326, ESO86SC38, KMHK1493	C	$5^{\mathrm{h}}53^{\mathrm{m}}52\overset{\mathrm{s}}{.}36$	$-63°36'50\overset{''}{.}9$	$47''$
OGLE-LMC-CL-0981	LMC600.20	OHSC27, KMHK1469/BSDL3145	C/CA	$5^{\mathrm{h}}52^{\mathrm{m}}29\overset{\mathrm{s}}{.}93$	$-63°36'03\overset{''}{.}5$	$34''$
OGLE-LMC-CL-0982	LMC600.21	NGC2120, SL742, LW316, ESO86SC34,	C	$5^{\mathrm{h}}50^{\mathrm{m}}35\overset{\mathrm{s}}{.}23$	$-63°40'58\overset{''}{.}8$	$45''$
⋮	⋮	⋮	⋮	⋮	⋮	⋮
OGLE-LMC-CL-1414	LMC520.31	BSDL1780	AC	$5^{\mathrm{h}}27^{\mathrm{m}}39\overset{\mathrm{s}}{.}14$	$-64°36'33\overset{''}{.}7$	$53''$
OGLE-LMC-CL-1415	LMC520.32	LW212,KMHK882/BSDL1630	C/C	$5^{\mathrm{h}}26^{\mathrm{m}}09\overset{\mathrm{s}}{.}45$	$-64°33'34\overset{''}{.}7$	$33''$
OGLE-LMC-CL-1416	LMC520.32	BSDL1654	A	$5^{\mathrm{h}}26^{\mathrm{m}}38\overset{\mathrm{s}}{.}81$	$-64°26'08\overset{''}{.}9$	$31''$
OGLE-LMC-CL-1417	LMC596.16	DES001SC14	–	$5^{\mathrm{h}}35^{\mathrm{m}}12\overset{\mathrm{s}}{.}87$	$-64°37'22\overset{''}{.}2$	$53''$
OGLE-LMC-CL-1418	LMC596.29	DES001SC18	–	$5^{\mathrm{h}}40^{\mathrm{m}}41\overset{\mathrm{s}}{.}98$	$-63°49'07\overset{''}{.}4$	$41''$
OGLE-LMC-CL-1419	LMC592.13	DES001SC07	–	$5^{\mathrm{h}}28^{\mathrm{m}}44\overset{\mathrm{s}}{.}41$	$-64°03'24\overset{''}{.}7$	$41''$
OGLE-LMC-CL-1420	LMC592.17	DES001SC11	–	$5^{\mathrm{h}}35^{\mathrm{m}}05\overset{\mathrm{s}}{.}67$	$-63°32'17\overset{''}{.}7$	$38''$
OGLE-LMC-CL-1421	LMC592.28	DES001SC09	–	$5^{\mathrm{h}}31^{\mathrm{m}}49\overset{\mathrm{s}}{.}44$	$-63°19'19\overset{''}{.}7$	$39''$
OGLE-LMC-CL-1422	LMC592.28	DES001SC10	–	$5^{\mathrm{h}}31^{\mathrm{m}}20\overset{\mathrm{s}}{.}16$	$-63°26'00\overset{''}{.}5$	$63''$
OGLE-LMC-CL-1423	LMC520.23	DES001SC05	–	$5^{\mathrm{h}}27^{\mathrm{m}}41\overset{\mathrm{s}}{.}37$	$-64°48'26\overset{''}{.}1$	$51''$
OGLE-LMC-CL-1424	LMC520.26	DES001SC14	–	$5^{\mathrm{h}}35^{\mathrm{m}}13\overset{\mathrm{s}}{.}07$	$-64°37'22\overset{''}{.}3$	$52''$

Table 2 presents the OGLE collection of new star clusters. Column 1 contains the OGLE identification number, column 2 shows the field name, in columns 3 and 4 we list the equatorial coordinates (J2000) of cluster center, in column 5 the reliability index and the last column contains the radius of the cluster in arcseconds.

Table 3 presents the OGLE collection of star clusters, which were already known. We cross-matched our detections with the Bica catalog and the DES catalog. All but six clusters listed in those catalogs which are located in the analyzed area of the LMC were also found in OGLE data. The names in column 2 were taken mostly from the Bica catalog. The DES catalog (Pieres *et al.* 2016) contains only 28 objects which are cataloged by the authors as new ones. We identified 12 of them as listed in the Bica catalog as type AC (association similar to cluster) or A (association) objects. Thus we listed only 15 clusters as genuine DES new findings. DES001SC12 is located in the gap between OGLE-IV subfields so our algorithm did not detect it. Nevertheless, we include the DES names for all 27 clusters in column 3.

Column 1 contains the OGLE identification number, column 2 shows the field name. In column 3 we list the cross-identification of clusters, in column 4 is cluster type (C – ordinary cluster, CN – cluster in nebula, CA – cluster similar to association, A – ordinary association, AC – association similar to cluster). Columns 5 and 6 show our estimation of the equatorial coordinates (J2000) and column 7 shows our estimation of the radius in arcseconds. For all previously known clusters we calculated the reliability parameter equal to one, so we do not list their values here.

The catalog, the list of all analyzed LMC fields and the graphical materials are available on the OGLE web page and FTP archive:

http://ogle.astrouw.edu.pl
ftp://ftp.astrouw.edu.pl/ogle/ogle4/clusters/lmc

5. Conclusions

We have presented a catalog of star clusters in the outer regions of the Large Magellanic Cloud based on the OGLE-IV deep photometric maps. We found a total of 679 star clusters, including 226 new objects which were not listed in any of the previous catalogs, 438 clusters listed in Bica *et al.* 2008 and 15 objects listed in the Dark Energy Survey publication (Pieres *et al.* 2016). For all of them the equatorial coordinates and cross-identification with previous catalogs are provided. The detection method presented in this paper is very effective. With our algorithm we found almost all previously known clusters in this characteristic sparse region of the LMC and increased the total number of these objects by 50%. This paper is the first of a series of publications. In the coming papers we will present a complete catalog of star clusters in the whole Magellanic System with their parameters determined, for the first time, from a single, homogeneous photometric data set collected by the OGLE project.

Acknowledgements. We would like to thank Profs. M. Kubiak and G. Pietrzyński, former members of the OGLE team, for their contribution to the collection of the OGLE photometric data over the past years.

We gratefully acknowledge the financial support of the Polish National Science Center, grant SONATA 2013/11/D/ST9/03445 to D. Skowron. Z. Kostrzewa-Rutkowska acknowledges support from European Research Council Consolidator Grant 647208. The OGLE project has received funding from the National Science Center, Poland, grant MAESTRO 2014/14/A/ST9/00121 to A. Udalski.

REFERENCES

Bhatia, R.K., and MacGillivray, H.T. 1989, *A&A*, **211**, 9.
Bica, E., Bonatto, C., Dutra, C.M., and Santos, J.F.C. 2008, *MNRAS*, **389**, 678.
Choudhury, S., Subramaniam, A., and Piatti, A.E. 2015, *AJ*, **149**, 52.
Cioni, M.-R.L., Habing, H.J., and Isreal, F.P. 2000, *A&A*, **358**, 9.
Deb, S., and Singh, H.P. 2014, *MNRAS*, **438**, 2440.
Glatt, K., Grebel, E.K., and Koch, A., 2010, *A&A*, **517**, A50.
Jacyszyn-Dobrzeniecka, A., *et al.* 2016, *Acta Astron.*, **66**, 149.
Klein, C.R., Cenko, S.B., Miller, A.A., Norman, D.J., and Bloom, J.S. 2014, arXiv1405.1035.
Nayak, P.K., Subramaniam, A., Choudhury, S., Indu, G., and Sagar, R. 2016, *MNRAS*, in press.
Palma, T., Gramajo, L.V., Claria, J.J., Lares, M., Geisler, D., and Ahumada, A.V. 2016, *A&A*, **586**, A41.
Piatti, A.E., Sarajedini, A., Geisler, D., Bica, E., and Claria, J.J. 2002, *MNRAS*, **329**, 556.
Piatti, A.E., Geisler, D., Bica, E., and Claria, J.J. 2003a, *MNRAS*, **343**, 851.
Piatti, A.E., Bica, E., Geisler, D., and Claria, J.J. 2003b, *MNRAS*, **344**, 965.
Piatti, A.E., Geisler, D., Sarajedini, A., and Gallart, C. 2009, *A&A*, **501**, 585.
Piatti, A.E., *et al.* 2014, *A&A*, **570**, A74.
Piatti, A.E., *et al.* 2015, *MNRAS*, **454**, 839.
Pieres, A., *et al.* 2016, *MNRAS*, **461**, 519.
Pietrzyński, G., Udalski, A., Kubiak, M., Szymański, M.K., Woźniak, P., and Żebruń, K. 1999, *Acta Astron.*, **49**, 521.
Pietrzyński, G., and Udalski, A. 2000, *Acta Astron.*, **50**, 337.
Schechter, P.L., Mateo, M., and Saha, A. 1993, *PASP*, **105**, 1342.
Scowcroft, V., Freedman, W.L., Madore, B.F., Monson, B.F., Monson, A., Persson, S.E., Rich, J., Seibert, M., and Rigby, J.R. 2016, *ApJ*, **816**, 49.
Skowron, D.M., *et al.* 2014, *ApJ*, **795**, 108.
Udalski, A., Kubiak, M., and Szymański, M.K., 1997, *Acta Astron.*, **47**, 319.
Udalski, A., Szymański, M.K., Soszyński, I., and Poleski, R. 2008, *Acta Astron.*, **58**, 69.
Udalski, A., Szymański, M.K., and Szymański, G. 2015, *Acta Astron.*, **65**, 1.
Zaritsky, D., Harris, J., and Thompson, I. 1997, *AJ*, **114**, 1002.